Superspin glass originating from dipolar interaction with controlled interparticle distance among γ-Fe_2O_3 nanoparticles with silica shells

Kosuke Hiroi,[1] Katsuyoshi Komatsu,[2,*] and Tetsuya Sato[1]

[1]*Department of Applied Physics & Physico-Informatics, Faculty of Science and Technology, Keio University, Yokohama, 223-8522, Japan*

[2]*Service de Physique de l'Etat Condensé, CEA Saclay, F-91191 Gif/Yvette Cedex, France*

(Received 24 February 2011; revised manuscript received 21 April 2011; published 28 June 2011)

γ-Fe_2O_3/SiO_2 core-shell nanoparticles with different shell thicknesses were prepared to elucidate the condition for superspin-glass (SSG) dynamics. As the shell thickness decreases, the contribution of interparticle dipolar interaction becomes apparent in the magnetic dynamics of nanoparticle assembly. The frequency dependence of peaks in ac-magnetic susceptibility in samples with strong interactions slows down, which is characterized as the emergence of a spin-glasslike phase. Aging in magnetization relaxation is found in a strongly interacting sample with an interparticle distance of $L \leqslant 14$ nm but is scarce in a sample with $L = 18$ nm. Scaling analysis reveals an increase in superparamagnetic properties with an increase in L. Therefore the critical interparticle distance necessary for SSG transition is 15–18 nm with 11-nm γ-Fe_2O_3 nanoparticles. This corresponds to the ratio of interparticle-interaction energy to the magnetic-anisotropy energy $E_{\mathrm{dip}}/E_{\mathrm{a}}$ of 6–12%.

DOI: 10.1103/PhysRevB.83.224423 PACS number(s): 75.50.Tt, 75.50.Lk, 75.10.Nr, 75.20.−g

I. INTRODUCTION

Single-domain magnetic nanoparticles called superspins have attracted a great deal of attention for the last few decades as promising materials for ultrahigh density-magnetic recording, e.g., patterned media.[1] In such an application single-domain magnetic islands, i.e., magnetic dipoles or superspins, are used as recording bits, and thus individually responding magnetic bits are required. However, it is difficult to satisfy this requirement in the dense magnetic-nanoparticle system because the dipolar interaction becomes very strong as the particle concentration increases. In such a strongly interacting nanoparticle system, collective phenomena have been reported.[2]

In a very dilute magnetic nanoparticle system the magnetic dynamics in the superparamagnetic framework can be well explained in terms of the Néel-Brown expression,[3] as follows:

$$\tau = \tau_0 \exp\left[\frac{E_a}{k_B T}\right], \tag{1}$$

where the flipping time τ of the magnetic moment of a nanoparticle is governed by its anisotropy energy E_{a} and a given temperature T, where τ_0 is on the order of 10^{-9}–10^{-12} s and k_{B} is the Boltzmann constant. In the high-temperature regime $E_{\mathrm{a}} \ll k_{\mathrm{B}}T$, the magnetic moments of the nanoparticles thermally fluctuate, and the magnetic behaviors coincide with Curie's law. On the other hand, with decreasing temperature, the magnetic moment of a nanoparticle is fixed along its easy axis as the anisotropy-energy barrier cannot be thermally exceeded. Because of this blocking phenomenon the superparamagnetic magnetization exhibits a peak at a certain temperature T_{peak}, below which it decreases as the temperature decreases. T_{peak} is the characteristic temperature below which the system changes from the paramagnetic state to the blocked state, and it is related to the blocking temperature as follows:

$$T_B = \frac{E_a}{k_B \ln(\tau/\tau_0)}. \tag{2}$$

In concentrated particle systems the particles' magnetic behavior is significantly influenced by interparticle interactions. The magnetic behavior of such systems has been actively studied using a frozen state of ferrofluid where magnetic particles are dispersed in carrier liquids and affected by the dipolar interaction. There have been many reports that the anisotropic-energy barrier in interacting particle systems increases with interparticle interaction, and that the blocking temperature is higher than that in an isolated particle system.[4,5] In 1988 Dormann *et al.*[6] proposed a model in which the interaction energy E_{int} is added to the energy barrier E_{a} in the expression of superparamagnetic relaxation time τ as follows:

$$\tau = \tau_0 \exp\left[\frac{E_a + E_{\mathrm{int}}}{k_B T}\right]. \tag{3}$$

This model is called the Dormann-Bessais-Fiorani model (DBF model).

On the other hand, the Mössbauer spectroscopy study of weakly interacting γ-Fe_2O_3 nanoparticles[7] showed that the relaxation time decreases as the interparticle-interaction increases. Mørup *et al.*[8] explained this experimental observation using a model in which the effective energy barrier decreases with increasing interaction energy at low temperatures within a weakly interacting region [Mørup-Tronc (MT) model].

Many studies show that a highly concentrated nanoparticle assembly exhibits a phase transition from a superparamagnetic state to a collective state at low temperature.[9,10] This magnetic phase is caused by the frustration of interparticle interaction that is induced by randomness in particle positions and anisotropy-axes orientations. This state is called superspin glass (SSG)[11] based on an analogy with spin glass in the magnetic state characterized by randomness and frustration, as observed in dilute magnetic alloys, e.g., AuFe,[12] AgMn,[13] and CuMn.[14] SSG exhibits slow dynamics at low temperatures

that are similar to the dynamics of spin glasses, i.e., aging phenomena,[15] memory effect, and weak rejuvenation.[16,17] In the dense nanoparticle systems used in the study of SSG, i.e., frozen-concentrated ferrofluid[18] and some granular films,[19] the interparticle distance and particle geometry are completely random, and there is a possibility of particle agglomeration. This makes estimating the interparticle distance and thus the strength of dipolar interaction difficult. For these reasons the origin of spin-glasslike phenomena in SSG has not been clearly understood.

Recently, with progress in the development of a method to chemically synthesize nanostructured materials, there have been many reports on core-shell nanostructures coated with uniform shells.[20,21] As a result, we can prepare magnetic particles with nonmagnetic shells with controlled thickness and thus assemble nanoparticles with a controlled interparticle distance through a bottom-up approach. In the present study we prepared silica-coated magnetic nanoparticles to make assemblies of magnetic nanoparticles whose interparticle distance could be systematically controlled. In such nanocomposites (NC), particle agglomeration is perfectly prevented, and the dipolar interaction can be directly evaluated through the silica-shell thickness. We used γ-Fe_2O_3 nanoparticles for which glassy behavior has been reported at low temperatures in concentrated colloidal dispersions.[15] To observe SSG behaviors we performed dynamic-scaling analysis based on the real part of ac magnetization[22] and observed the aging phenomena that are characteristic of SSG using the zero-field-cooling (ZFC) protocol.[23]

II. EXPERIMENTAL PROCEDURE

A synthetic method of monodispersed nanoparticles of γ-Fe_2O_3 capped with oleic acid is described in Hyeon *et al*. (2001).[24] We performed silica coating of the synthesized nanoparticles by reverse microemulsion.[25] Figure 1(a) shows a transmission electron microscopy (TEM) image of γ-Fe_2O_3 nanoparticles. The fitting of the diameter histogram to a lognormal-distribution function yields the average diameter D_{ave} of 11 nm and the volume distribution σ_V of 0.24. We prepared γ-Fe_2O_3/SiO_2 NCs with various SiO_2-shell thicknesses [Figs. 1(b)–1(d)]. Table I shows the correspondence list of sample names and the interparticle distances of each sample. We realized seven kinds of interparticle distances among six kinds of NC samples and nanoparticles without SiO_2 shells that were capped with only oleic acid. In the samples for magnetic measurement the magnetic particles were aggregated and in a nearly closed-packed structure, so the interparticle distance was intrinsically determined based on the thicknesses of the SiO_2 shell or oleic-acid layer. All measurements were performed using a commercial, superconducting quantum-interference device magnetometer (Quantum Design, MPMS-XL with ultralow-field option). The magnetic moment of the single γ-Fe_2O_3 nanoparticle $m = 2.3 \times 10^4\ \mu_B$ was evaluated from the fitting of the magnetization curve of a superparamagnetic sample with the thickest SiO_2 coating (L47) to the Langevin function. This is consistent with the other reports on the γ-Fe_2O_3 nanoparticle.[26]

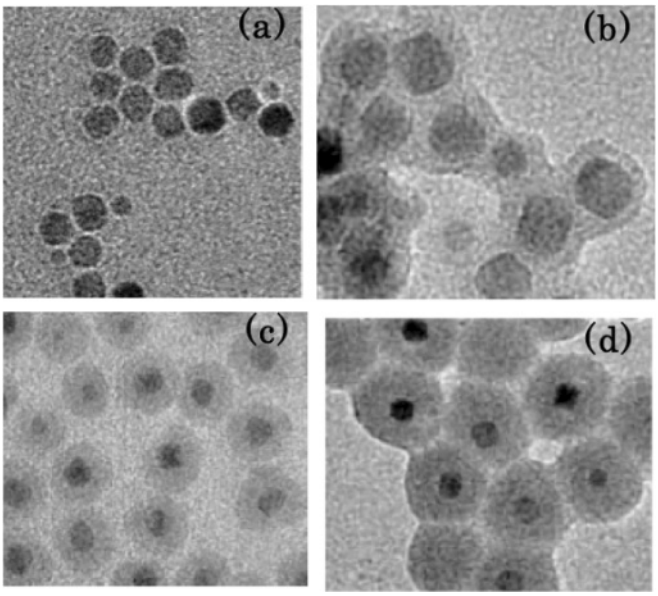

FIG. 1. (a) TEM images of γ-Fe_2O_3 NPs ($D_{ave} = 11$ nm), (b) NCs with $L = 18$ nm, (c) $L = 26$ nm, and (d) $L = 34$ nm.

TABLE I. Interparticle distance in each sample.

Sample name	L12	L14	L18	L26	L30	L34	L47
L [nm]	12	14	18	26	30	34	47

III. EXPERIMENTAL RESULTS

A. Dc magnetization

Figure 2 shows the temperature-dependent magnetization of each sample. Magnetizations are normalized with the value at T_{peak} in ZFC magnetization. With increasing the SiO_2-shell thickness of the sample, T_{peak} is lowered and the low-temperature increase in field-cooled (FC) magnetization becomes pronounced. These features are observed in conventional superparamagnetic nanoparticle systems in which the interparticle interaction is very small. T_{peak} rises with shortening the interparticle distance. In the most concentrated sample, L12, the low-temperature FC magnetization shows no increase but rather a slight decrease, which has often been

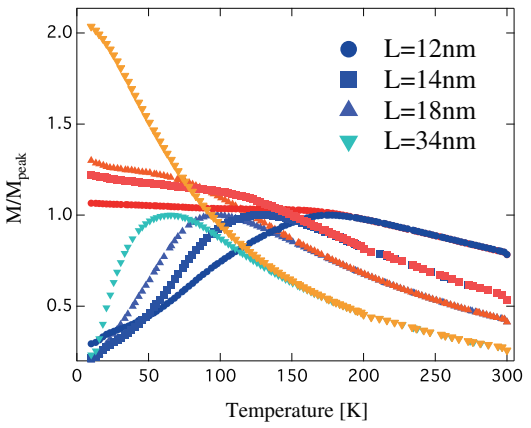

FIG. 2. (Color online) Temperature-dependent magnetization of the samples L12, L14, L18, and L34 under ZFC and FC conditions. All curves are normalized by the value in T_{peak} in the ZFC condition.

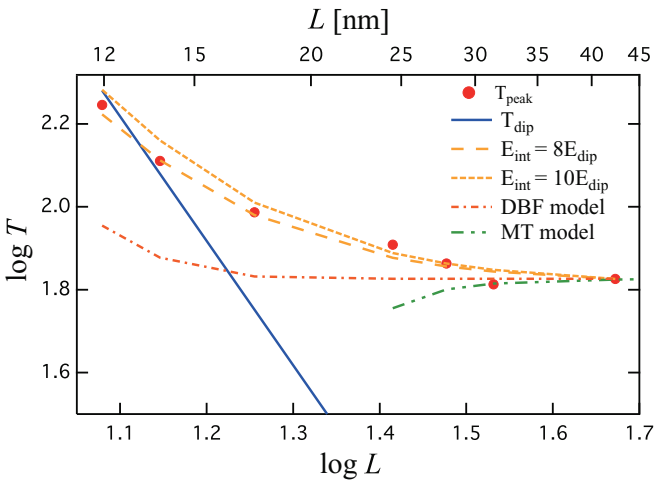

FIG. 3. (Color online) Log-log plot of T_{peak} in the dc susceptibility as a function of the interparticle distance L. The solid line indicates the dipole-dipole interaction between magnetic particles. The dashed lines are the qualitatively explained lines with $E_{int} = 8E_{dip}$ and $10E_{dip}$. The dashed-dot curves are calculations using the DBF model ($E_{int} = E_{dip}L[E_{dip}/k_BT_{peak}]$) and the MT model ($\sum_j a_{ij}^{-6} = 20$).

observed in other SSG.[2] These results are consistent with many experimental observations that T_{peak} shifts toward the higher temperature because of the influence of interparticle interaction.[4,5]

Figure 3 shows log T_{peak} as a function of log L. The solid line represents the strength of dipolar interaction as $T_{dip} = E_{dip}/k_B$. The value of E_{dip} between neighboring particles is approximated as follows:

$$E_{dip} = \frac{\mu_0 m^2}{4\pi L^3}, \tag{4}$$

where m is the magnetic moment of the particle and μ_0 is the permeability of a vacuum. Based on Eq. (4) the slope of -3 should be observed for T_{dip} in logarithmic plots. In Fig. 3 we subsequently pay attention to T_{peak} in order from the sample with long interparticle distance. For L34 and L47 that have very large L, T_{peak} for smaller L is low, although the change is subtle. In samples L18–L30, however, T_{peak} slightly increases with decreasing L. The L dependence of T_{peak} is expressed by $T_{peak}\ L^{-0.6}$ for L18–L30, which is consistent with that of the Fe_3O_4/SiO_2 core-shell nanoparticle in Yang *et al.* (2009).[25] In samples L12 and L14 the L dependence of T_{peak} is very close to that of T_{dip} as expected in the SSG, as will be discussed in Sec. IV C. This indicates that the magnetic nature of L12 and L14 may be categorized as SSG. In the following paragraphs we classify samples as follows: L12–L18 in the strongly interacting region, L18–L34 in the weakly interacting region, and L47 in a superparamagnetic region with negligibly weak interparticle interaction.

B. Ac-magnetic susceptibility

To investigate magnetic dynamics in more detail, we measured ac-magnetic susceptibility of samples L12–L18, which are expected to be very close to SSG according to dc measurement, in addition to L47, which is supposed to exhibit superparamagnetism with negligibly weak interaction.

First ac-magnetic susceptibility of the superparamagnetic sample L47 was measured with a driving field 1 Oe. Figure 4

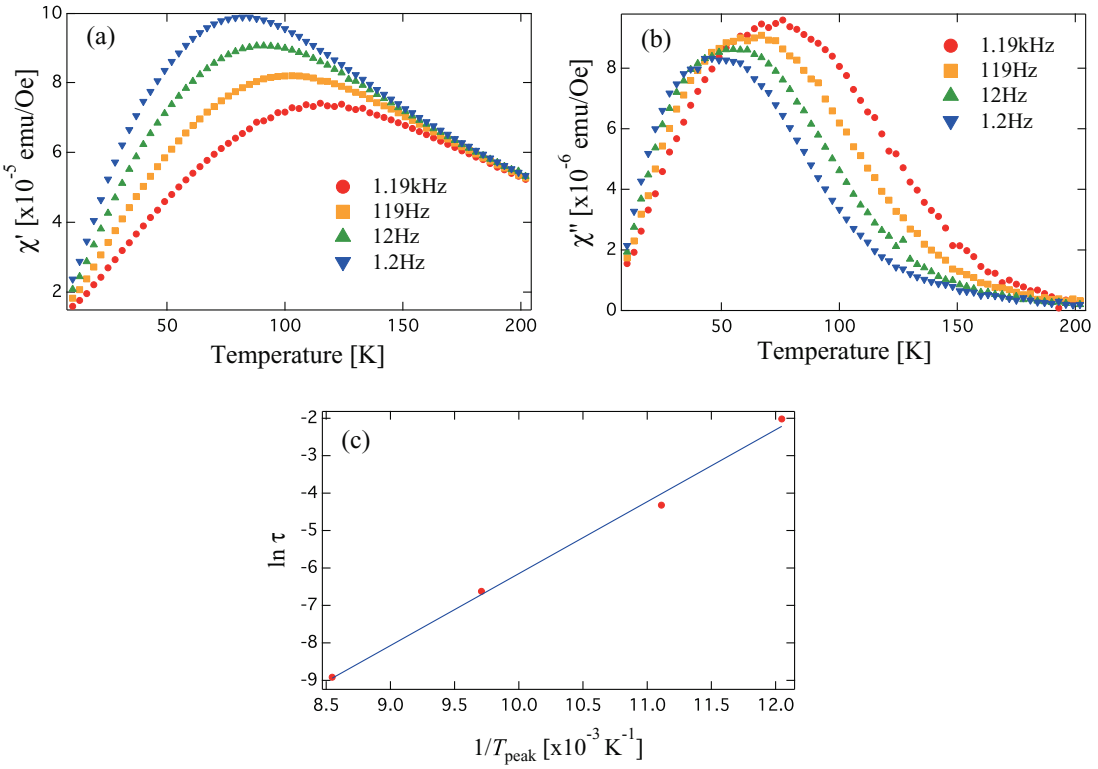

FIG. 4. (Color online) (a) In-phase and (b) out-of-phase ac magnetizations of L47 at frequencies of 1.2, 12.0, 119, and 1190 Hz. (c) Arrhenius law fit to ln τ versus $1/T_{peak}$.

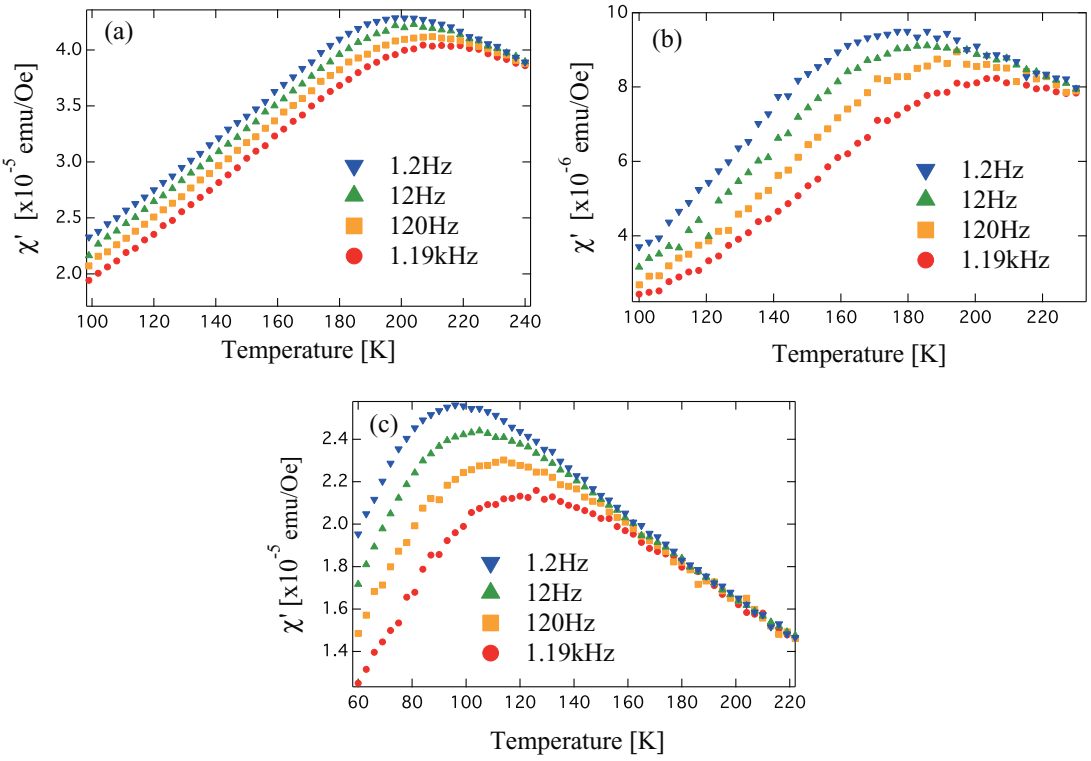

FIG. 5. (Color online) In-phase ac magnetization of samples (a) L12, (b) L14, and (c) L18 at frequencies of 1.19 kHz, 120 Hz, 12 Hz, and 1.2 Hz.

shows the in-phase and out-of-phase ac-magnetic susceptibility. The temperatures at which the in-phase and out-of-phase ac-magnetic susceptibilities exhibit their peaks increase with increasing frequency. $T_{\rm peak}$ in out-of phase ac magnetization corresponds to the blocking temperature $T_{\rm B}$.[28] Using Eq. (1) with observation time $\tau = 1/(2\pi f)$ (f being the measuring frequency) and $T_{\rm B}$, the anisotropy energy $E_{\rm a} = 1.4 \times 10^{-20}$ J and $\tau_0 = 1.6 \times 10^{10}$ s is obtained [Fig. 4(c)]. These values for γ-Fe_2O_3 nanoparticles are comparable to those in another report.[29]

On the other hand the magnetic dynamics of samples L12–L18 in the strongly interacting region should be close to that of spin glass. If these samples exhibit glassy dynamics at low temperatures, the following relation of critical slowing down would be expected around transition temperature $T_{\rm c}$[22]:

$$\frac{1}{2\pi f} = \tau^* \left[\frac{T_{\rm peak}^{AC} - T_c}{T_c} \right]^{-z\nu}, \qquad (5)$$

where $T_{\rm peak}^{AC}$ is the temperature at which the in-phase ac-magnetic susceptibility exhibits its peak, τ^* is a relaxation time of each nanoparticle, and $z\nu$ is a dynamic-critical exponent. Figure 5 shows the in-phase ac-magnetic susceptibility for L12–L18. We determined $T_{\rm c}$ and $z\nu$ as fitting parameters based on the $\log(1/2\pi f)$ versus $T_{\rm peak}^{AC}$ plots to obtain the best fit to Eq. (5). Figure 6 shows the log-log plot of $1/2\pi f$ versus $(T_{\rm peak}^{AC} - T_c)/T_c$, from which the parameters were obtained for L12–L18. The value of $z\nu \sim 10$, which is obtained for all the samples classified in the strongly interacting region and is very close to the reported values in the other SSGs.[30]

C. Magnetic-aging phenomena

To observe glassy dynamics at low temperatures, we observed the magnetic relaxation below $T_{\rm c}$. Such a magnetic-aging phenomenon of the relaxation rate should be observed in SSG. In spin glasses, magnetic relaxation measured below $T_{\rm c}$ depends on the waiting time before measurement. The measurement procedure is as follows: The sample is first cooled to a certain temperature $T_{\rm ob}$ ($<T_{\rm c}$) at a constant cooling rate of 5 K/min in zero field. When the temperature reaches $T_{\rm ob}$, the probing field of 1 Oe is applied after the waiting time $t_{\rm w}$. Then the inflection point appears in time-dependent magnetization at a time almost equal to $t_{\rm w}$.[31] This is clearly visualized as a peak in the relaxation rate $S(t) = dM(t)/d\log t$. Figure 7 shows the time dependence of $S(t)$. All the measurements are performed at a sufficiently low temperature below $T_{\rm c}$ ($\sim$0.5 $T_{\rm peak}$). For L12 and L14, $S(t)$ clearly exhibits the waiting-time dependence. However, the aging behavior in L14 is rather noisy compared with that in L12. Aging behavior is not observed in L18, even though the obtained critical exponent is consistent with that of SSG in dynamic-scaling analysis. These results indicate that clear aging behavior is only observed in the samples with strong interparticle interactions with $L \leqslant 14$ nm.

IV. DISCUSSION

A. Superparamagnetic region

Figure 3 shows that in samples L34 and L47, $T_{\rm peak}$ in the ZFC magnetization is scarcely dependent on interparticle distance. The dipolar-interaction energy in L47 is 1% or less of anisotropy energy of the γ-Fe_2O_3 nanoparticle, and thus

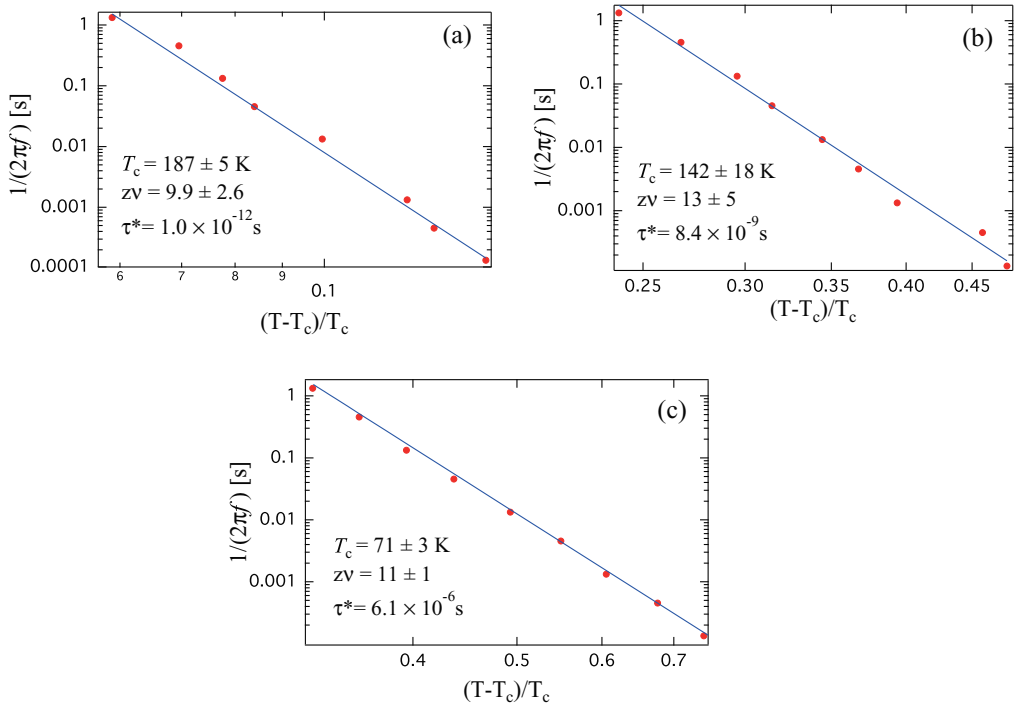

FIG. 6. (Color online) $1/(2\pi f)$ versus $(T_{peak} - T_c)/T_c$ plotted on log-log scale for (a) L12, (b) L14, and (c) L18.

the contribution of dipolar interaction is negligibly small for the magnetic dynamics of NC assembly. According to Mamiya *et al.*,[32] T_{peak} is almost proportional to the blocking temperature T_B in the superparamagnetic regime, and the ratio of T_{peak} to T_B is almost irrelevant to the measurement time as long as the size distribution of the particle and the applied field are unchanged. Therefore T_{peak} and T_B behave similarly in the superparamagnetic region. Based on the studies by Mamiya *et al.*, the ratio of T_{peak} to the average blocking temperature $\langle T_B \rangle$, $T_{peak}/\langle T_B \rangle$, is 1.4–1.5 under the condition of the volume distribution σ_V of 0.24 for the γ-Fe_2O_3 nanoparticles used in this study. Thus $\langle T_B \rangle$ of 45 K–48 K is estimated for L47. This corresponds to $E_a = 1.6$–1.7×10^{-20} J using Eq. (2), which is consistent with $E_a = 1.4 \times 10^{-20}$ J obtained by the ac measurement.

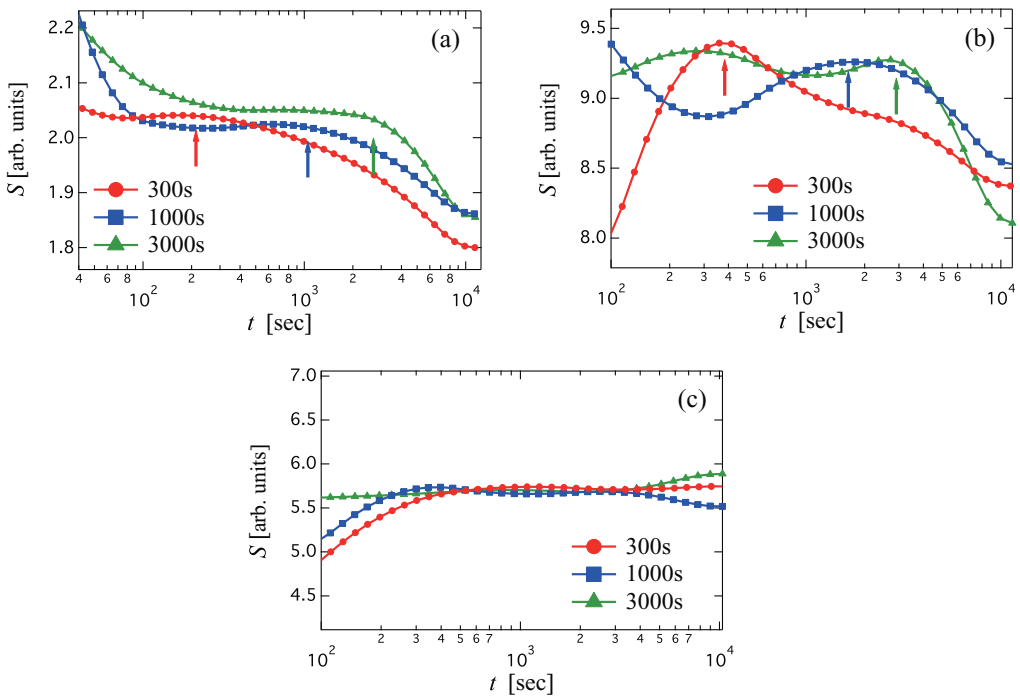

FIG. 7. (Color online) Time dependence of relaxation rate of samples (a) L12, (b) L14, and (c) L18 with waiting times 300 s, 1000 s, and 3000 s.

B. Weakly interacting region

The changes in T_{peak} ($\sim$1.5 T_B) for L18–L30, depending on interparticle distance, are qualitatively consistent with the DBF model. In this model the spin dynamics are determined by Eq. (3), in which the interaction energy E_{int} is effectively added to the anisotropy energy E_a. By comparing the increments in anisotropy energy E_{int} in Eq. (3) with the dipole interaction energy E_{dip} between neighboring particles, we can quantitatively explain the shifts of T_{peak} using $E_{int} = nE_{dip}$ with $n = 8$–10, as shown in Fig. 3. However, Dormann *et al.* define E_{int} as

$$E_{int} \sim N \cdot E_{dip} L\left[\frac{E_{dip}}{k_B T}\right], \tag{6}$$

where N is the number of neighboring particles and $L[\ldots]$ is the Langevin function. We cannot quantitatively explain shifts of T_{peak} by the DBF model because the value of the Langevin function estimated from $L[E_{dip}/k_B T_{peak}]$ is 0.34–0.055 for L12–L30.

On the other hand T_{peak} of L34 is lower than that of L47, which is not consistent with the DBF model but is consistent with the MT model,[8] in which the blocking temperature is lowered with increasing the interparticle interaction in a weakly interacting region. Mørup *et al.* evaluated the average square-mean dipolar field $\langle H_{dip}^2 \rangle$ caused by surrounding particles in a way similar to the method used by van Vleck[33] for a magnetic ion in paramagnetic materials and obtained

$$E_{dip}^2 = m^2 \cdot H_{dip}^2 = 2E_{dip}^2 \sum_j a_{ij}^{-6}. \tag{7}$$

The sum of α_{ij} depends on the geometrical arrangement of the particles, and Mørup *et al.* estimated $\sum_j a_{ij}^{-6} \sim$10–20. The difference of T_{peak} between L47 and L34 is consistent with this model with $\sum_j a_{ij}^{-6} = 20$. The lowering of T_{peak} with decreasing L is observed only in L47 and L34. When the interparticle interaction is further strengthened from L34 to L18, T_{peak} increases. This is because the dipolar interaction is too strong and exceeds the limit of application of the MT model. Mørup *et al.* indicate that the model is applicable under the condition of interparticle interaction $\beta = E_{dip}/k_B T \ll 1$. Using the approximate expression $\beta \sim E_{dip}/k_B T_{peak}$, we can evaluate $\beta \sim 0.13$ in L34, and β varies from 0.17 to 0.58 among the samples L30–L18. Based on the present result the MT model is applicable only in a very weak interacting region of $\beta < 0.13$, and the increase in E_{dip} over this range induces an increase in T_{peak}.

C. Strongly interacting region

In a strongly interacting region where magnetic ordering occurs from the interparticle-dipolar interaction, T_{peak} should be related to the transition temperature T_c, which is related to E_{dip} as

$$T_c = a_0 \frac{E_{dip}}{k_B}, \tag{8}$$

where a_0 is the parameter that makes the connection between T_c and E_{dip}.[34] Mørup emphasizes that this expression is valid even in the system with nonuniform-interparticle distance. Therefore the value of T_c, obtained by dynamic-scaling analysis, should depend on E_{dip} according to Eq. (6). Using the values of T_c and T_{dip} evaluated in the present study, $a_0 = 0.86$ is obtained. In the recent Monte Carlo simulations[35] the relation $a_0 = (0.96 \pm 0.07)x$ was predicted, where x is the site occupancy rate, i.e., the probability that a lattice site is occupied by a dipole. The value of x, estimated from the dynamic-scaling analysis, is $0.86/0.96 = 0.9$. This indicates that nanoparticles are not perfectly close packed in our powder sample because perfectly close-packed nanoparticles with super-lattice structures[36] have the site occupancy rate $x = 1$. Thus the packed-powder sample used in the present work does not form a superlattice structure, and the number of neighboring particles is 10–11. This value is very close to $n = E_{int}/E_{dip}$, as estimated previously. Therefore n should be comparable to the number of neighboring particles N.

The relaxation time of each particle τ^* in Eq. (5), which is obtained in the dynamic-scaling analysis, increases with increasing interparticle distance, as shown in Fig. 6. This is because the temperature range in which the dynamic-scaling analysis is performed shifts to low temperature with increasing interparticle distance, and the relaxation time depends on the temperature, as described in Eq. (1). Based on τ_0 and E_a, which is evaluated from the ac data of superparamagnetic sample L47, the relaxation time τ of each particle is 2–4 $\times$ 10^{-8} and 3 $\times$ 10^{-7}–4 $\times$ 10^{-6} s for L14 and L18 at the corresponding temperatures, respectively. These values almost agree with τ^* obtained by dynamic-scaling analysis and is consistent with the previous report indicating that the two relaxation times are intrinsically the same.[30] Concerning L12, however, $\tau^* \sim 1 \times 10^{-12}$ s is rather smaller than τ of 1–3 $\times$ 10^{-8} s, even when a large margin of error is considered because the margin of error in fitting of τ^* for L12 is $\Delta \ln\tau^* = \pm 3.4$, indicating 3.4×10^{-14} s $< \tau^* < 3.1 \times 10^{-11}$ s.[37] Such a disagreement between τ^* and τ has also been observed in another report,[4] which indicates that strong interparticle interaction can modify the relaxation time of a single particle.

In addition to the interparticle-interaction dependence of T_c, the aging behavior is changed depending on E_{dip}. The waiting-time dependence of the peak position of the relaxation rate clearly appears in the strongly interacting sample L12. Such an aging behavior is also observed in L14, but the characteristics of the relaxation-rate curves become ambiguous and the waiting-time dependence of the peak position is not clear compared with L12. For L18 the relaxation rate scarcely depends on the waiting time, although the dynamic-scaling exponent is consistent with that of SSG. The absence of t_w dependence may be attributed to low resolution in the observation of aging phenomena in sample L18 because of the insufficient amount of the sample to allow detection of the detailed change in the relaxation rate.

Recently, Parker *et al.*[38] reported that there is a superparamagnetic component in the relaxation in magnetization of SSG. To obtain a better understanding of the aging effect, we used the proposed scaling analysis. In atomic spin glasses, relaxation curves in zero field are expressed as the sum of

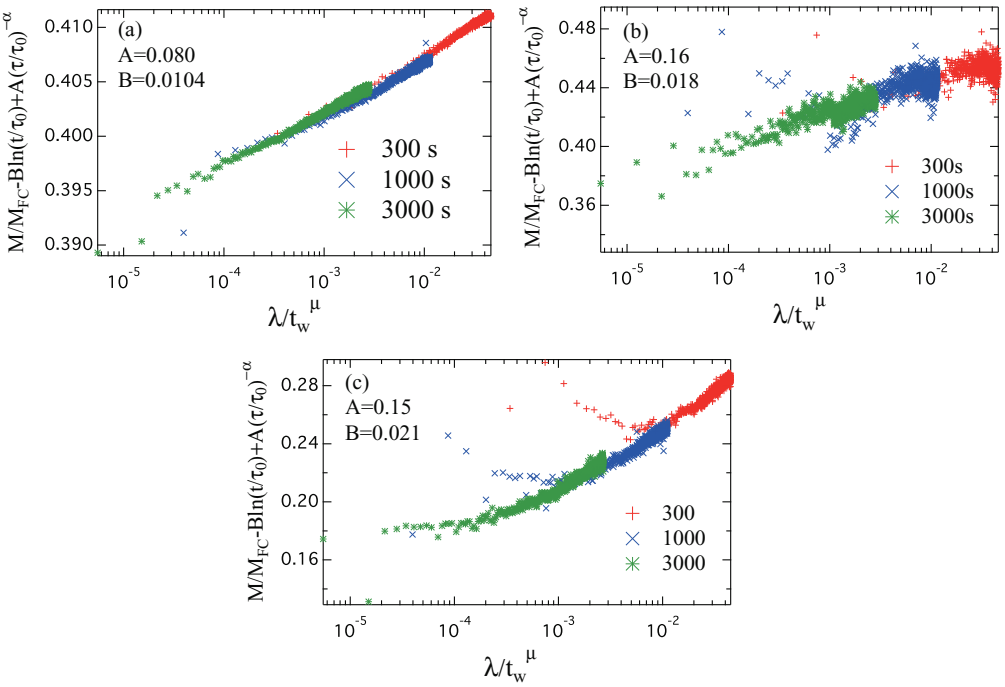

FIG. 8. (Color online) Scaling of the ZFC magnetization (a) L12, (b) L14, and (c) L18 where scaling exponents $\alpha = 0.085$ and $\mu = 0.9$ are used.

the stationary equilibrium part $m_{\rm eq}(t)$, and the aging part $m_{\rm ag}(t)$[39] as

$$\frac{M(t)}{M_{FC}} = m_{\rm ag}(t) + m_{\rm eq}(t) = f\left(\frac{t}{t_w^{\mu}}\right) - A\cdot\left(\frac{t}{\tau_0}\right)^{-\alpha}, \qquad (9)$$

where $M_{\rm FC}$ is the FC magnetization at $T_{\rm ob}$, A is the prefactor of an equilibrium part, f is the scaling function, and α and μ are the scaling exponents. Parker *et al.* extended this scaling law to the magnetic-particle system by adding superparamagnetic relaxation term $B\cdot\ln(t/\tau_0)$ and expressing the formula as follows:

$$\frac{M(t)}{M_{FC}} = f\left(\frac{t}{t_w^{\mu}}\right) - A\cdot\left(\frac{t}{\tau_0}\right)^{-\alpha} + B\cdot\ln(t/\tau_0). \qquad (10)$$

We subtracted $-A\cdot(t/\tau_0)^{-\alpha}$ and $B\cdot\ln(t/\tau_0)$ from M/M_{FC} and obtained the aging function $f(\lambda/t_w^{\mu})$. The variable $\lambda = t_w^{1-\mu}[(1+t/t_w)^{1-\mu}-1]/[1-\mu]$ is an effective time that accounts for the subaging[40] of the system, and μ of $\sim$0.9 is found for different types of spin glasses.[39] Figure 8 shows $f(\lambda/t_w^{\mu})$ and the fitted parameters A and B where the scaling exponents $\alpha = 0.085$ and $\mu = 0.9$, obtained in the other SSG,[38] are used. From the results of scaling, the amount of the superparamagnetic-relaxation term, $B\cdot\ln(t/\tau_0)$, is estimated to be 40–45% of the total relaxation of magnetization in L12. The superparamagnetic-relaxation term becomes significantly larger when the interparticle distance increases, i.e., 94–96% with L14 and 97–99% with L18. Parker *et al.*[38] explain this superparamagnetic term as a contribution of weakly interacting particles that are not coupled enough to their neighbors and show logarithmically slow relaxation toward equilibrium because of the anisotropy-energy barrier. In our case nanoparticles do not form superlattice structures, and thus the interparticle distance is not perfectly controlled and there exists inhomogeneity in the particle distance and the interaction strength. As a result, there may be some weakly interacting particles that behave like superparamagnetic particles in our samples.

It is interesting to note that the contribution of the superparamagnetic term becomes larger as the interparticle distance increases. This indicates that the amount of superparamagnetically contributing particles increases with thicker silica-shell samples. In other words, the contribution of the strongly coupled particles, which relax like spin glasses, to the magnetic relaxation decreases in the samples with longer interparticle distance. The number of weakly coupled particles that show the superparamagnetic behavior should rise as the average dipolar interaction in the system decreases. For this reason magnetic-aging phenomena in the relaxation rate are gradually smeared out as shell thickness increases and are scarcely observed in L18.

D. Contribution of randomness in the particle position

Two kinds of randomness in the particle position and easy axis orientation of a particle have been considered to be required for the appearance of SSG. In this study the interparticle distance was arranged in the definite value through the shell thickness in order to estimate the strength of interparticle interaction quantitatively. This should have resulted in a small degree of randomness in particle positions. Nevertheless, the results of this study are consistent with those of other studies that were performed using frozen ferrofluid in which there was significant randomness in particle positions. Furthermore it was recently reported that face-centered cubic supracrystals, which are composed of 8-nm-Co nanoparticles,

show SSG behaviors through the critical slowing down and memory effect.[41] These findings indicate that the contribution of randomness in easy axis orientations is dominant for the appearance of SSG compared with that of interparticle positions. To further specify the contribution of randomness to the appearance of SSG, detailed evaluation of the distribution of interparticle distance in the present powder samples in comparison with that in ferrofluid is required using high-resolution scanning electron microscopy and small-angle X-ray scattering.

E. Contribution of anisotropy of each particle

Many studies have demonstrated that the magnetic properties of the interacting-particle system are governed by the interplay of the single-particle anisotropy energy and the dipolar-interaction energy.[6,42,43] It has been indicated that SSG appears when the interparticle-dipolar interaction becomes significant, so that it cannot be neglected, compared with the anisotropy energy of each magnetic particle. However, to the best of our knowledge, there has been no report that specifies the strength of interaction needed to induce SSG. The present study results indicate that the strength of dipolar interaction at $L = 15$–18 nm is necessary to induce SSG corresponding to $E_{\mathrm{dip}} = 8$–15×10^{-22} J in γ-Fe_2O_3 nanoparticles with 11-nm diameter. This is about 10% of the anisotropy energy $E_{\mathrm{a}} = 1 \times 10^{-20}$ J. This evaluation of the relative dipolar interaction $E_{\mathrm{dip}}/E_{\mathrm{a}} \sim 0.1$ for SSG, based on highly reliable measurements, will be an important step to clarifying the freezing mechanism of ferromagnetic particles. However, we cannot specify whether the relative dipolar interaction is the predominant factor in the present stage because there may be other factors that govern the occurrence of SSG. Evaluation of relative dipolar interaction using other nanoparticle systems is required to better understand this issue. We have plans to perform similar measurements using other magnetic nanoparticles with higher anisotropy energy or larger saturation magnetization and compare our findings to the results of this study.

V. CONCLUDING REMARKS

We investigated the magnetic behavior of γ-Fe_2O_3/SiO_2 NCs with 11-nm diameter that were coated with SiO_2 to control the interparticle distance based on the thickness. The magnetic dynamics of particles with the thickest coating can be explained by the superparamagnetic model. The samples whose interparticle distance was shorter than 18 nm exhibited spin-glasslike behaviors where T_{peak} decreased with increasing of shell thickness, and the strong dipolar interaction induced SSG. The observation of the aging phenomena in the NCs whose interparticle distance was shorter than 14 nm indicated that the SSG arose at $L = 15$–18 nm. The ratio of dipolar interaction to anisotropy energy corresponding to $\sim$10% is necessary to induce SSG.

ACKNOWLEDGEMENT

This work was supported by the Keio University Doctoral Student Grant-in-Aid Program and the Grant-Aid for Doctoral Student Program from the Keio Leading-edge Laboratory of Science and Technology.

*Present address: Laboratoire de Physique des Solides, CNRS, UMR 8502, Univ. Paris-Sud, F-91405 Orsay, France.

[1] B. D. Terris and T. Thomson, J. Phys. D **38**, R199 (2005).
[2] O. Petracic, X. Chen, S. Bedanta, W. Kleemann, S. Sahoo, S. Cardoso, and P. P. Freitas, J. Magn. Magn. Mater. **300**, 192 (2006).
[3] W. F. Brown, Phys. Rev. **130**, 1677 (1963).
[4] M. F. Hansen, P. E. Jönsson, P. Nordblad, and P. Svedlindh, J. Phys. Condens. Matter **14**, 1 (2002).
[5] H. Mamiya, M. Ohnuma, I. Nakatani, and T. Furubayashi, Phys. Status Solidi (a) **201**, 3345 (2004).
[6] J. L. Dormann, L. Bessais, and D. Fiorani, J.Phys. C: Solid State Phys. **21**, 2015 (1988).
[7] P. Prené, E. Tronc, J. P. Jolivet, J. Livage, R. Cherkaoui, M. Noguès, J. L. Dormann, and D. Fiorani, IEEE Trans. Magn. **29**, 2658 (1994).
[8] S. Mørup and E. Tronc, Phys. Rev. Lett. **72**, 3278 (1994).
[9] W. Luo, S. R. Nagel, T. F. Rosenbaum, and R. E. Rosensweig, Phys. Rev. Lett. **67**, 2721 (1991).
[10] M. Suzuki, S. I. Fullem, I. S. Suzuki, L. Wang, and C. J. Zhong, Phys. Rev. B **79**, 024418 (2009).
[11] S. Bedanta and W. Kleemann, J. Phys. D: Appl. Phys. **42**, 013001 (2009).
[12] V. Cannella and J. A. Mydosh, Phys. Rev. B **6**, 4220 (1972).
[13] T. Taniguchi and Y. Miyako, J. Phys. Soc. Jpn. **57**, 3520 (1988).
[14] L. Sandlund, P. Granberg, L. Lundgren, P. Nordblad, P. Svedlindh, J. A. Cowen, and G. G. Kenning, Phys. Rev. B **40**, 869 (1989).
[15] T. Jonsson, J. Mattsson, C. Djurberg, F. A. Khan, P. Nordblad, and P. Svedlindh, Phys. Rev. Lett. **75**, 4138 (1995).
[16] K. Jonason, E. Vincent, J. Hammann, J. P. Bouchaud, and P. Nordblad, Phys. Rev. Lett. **81**, 3243 (1998).
[17] P. E. Jönsson, H. Yoshino, H. Mamiya, and H. Takayama, Phys. Rev. B **71**, 104404 (2005).
[18] T. Jonsson, P. Svedlindh, and M. F. Hansen, Phys. Rev. Lett. **81**, 3976 (1998).
[19] S. Sahoo, O. Petracic, W. Kleemann, P. Nordblad, S. Cardoso, and P. P. Freitas, Phys. Rev. B **67**, 214422 (2003).
[20] B. O. Dabbousi, J. Rodriguez-Viejo, F. V. Mikulec, J. R. Heine, H. Mattoussi, R. Ober, K. F. Jensen, and M. G. Bawendi, J. Phys. Chem. B **101**, 9463 (1997).
[21] D. C. Lee, F. V. Mikulec, J. M. Pelaez, B. Koo, and B. A. Korgel, J. Phys. Chem. B **110**, 11160 (2006).
[22] C. Djurberg, P. Svedlindh, P. Nordblad, M. F. Hansen, F. Bødker, and S. Mørup, Phys. Rev. Lett. **79**, 5154 (1997).
[23] P. Granberg, L. Sandlund, P. Nordblad, P. Svedlindh, and L. Lundgren, Phys. Rev. B **38**, 7097 (1988).
[24] T. Hyeon, S. S. Lee, J. Park, Y. Chung, and H. B. Na, J. Am. Chem. Soc. **123**, 12798 (2001).
[25] J. L. Gong, J. H. Jiang, Y. Liang, G. L. Shen, and R. Q. Yu, J. Colloid Interface Sci. **298**, 752 (2006).
[26] J. Zhang, C. Boyd, and W. Luo, Phys. Rev. Lett. **77**, 390 (1996).
[27] H. T. Yang, D. Hasegawa, M. Takahashi, and T. Ogawa, Appl. Phys. Lett. **94**, 013103 (2009).

[28]D. E. Madsen, M. F. Hansen, and S. Mørup, J. Phys. Condens. Matter **20**, 345209 (2008).
[29]F. Gazeau, J. C. Bacri, F. Gendron, R. Perzynski, Yu. L. Raikher, V. I. Stepanov, and E. Dubois, J. Magn. Magn. Mater. **186**, 175 (1998).
[30]P. Jönsson, M. F. Hansen, P. Svedlindh, and P. Nordblad, J. Magn. Magn. Mater. **226–230**, 1315 (2001).
[31]P. Granberg, L. Sandlund, P. Nordblad, P. Svedlindh, and L. Lundgren, Phys. Rev. B **38**, 7097 (1988).
[32]H. Mamiya, I. Nakayama, T. Furubayashi, and M. Ohnuma, Trans. Magn. Soc. Jpn. **2**, 36 (2002).
[33]J. H. van Vleck, J. Chem. Phys. **5**, 320 (1937).
[34]S. Mørup, Europhys. Lett. **28**, 671 (1994).
[35]J. F. Fernández and J. J. Alonso, Phys. Rev. B **79**, 214424 (2009).
[36]S. Sun, C. B. Murray, D. Weller, L. Folks, and A. Moser, Science **287**, 1989 (2000).
[37]We define the freezing temperature at which the system starts to deviate from the equilibrium dynamics as T_{peak} of in-phase susceptibility. As shown in the previous report (J. Phys.: Condens. Matter **14**, 4901 (2002)), however, there is another criterion for definition of freezing temperature; the freezing temperature is defined as the temperature at which $\chi' = 0.98\ \chi_{eq}$ (χ_{eq} is a equilibrium susceptibility). We also tried to perform the critical slowing down analysis using the temperature at which $\chi' = 0.96\ \chi_{eq}$ ($\sim 0.96\ \chi_{FC}$) and obtained $z\nu = 8.2 \pm 1.0$, $\tau^* = 1.9\text{–}61 \times 10^{-9}$ s with parameter T_c fixed at 180 K. The obtained small value of τ^* of L12 sample can be attributed to our criterion for definition of freezing temperature.
[38]D. Parker, V. Dupuis, F. Ladieu, J.-P. Bouchaud, E. Dubois, R. Perzynski, and E. Vincent, Phys. Rev. B **77**, 104428 (2008).
[39]V. Dupuis, F. Bert, J.-P. Bouchaud, J. Hammann, F. Ladieu, D. Parker, and E. Vincent, J. Phys. **64**, 1109 (2005).
[40]M. Ocio, M. Alba, and J. Hammann, J. Phys. (Paris) Lett. **46**, 1101 (1985).
[41]D. Parker, I. Lisiecki, and M. P. Pileni, J. Phys. Chem. Lett. **1**, 1139 (2010).
[42]D. Kechrakos and K. N. Trohidou, Phys. Rev. B **58**, 12169 (1998).
[43]D. Parker, I. Lisiecki, C. Salzemann, and M.-P. Pileni, J. Phys. Chem. C **111**, 12632 (2007).